Journal of Experimental Botany, Vol. 61, No. 4, pp. 1177–1192, 2010
doi:10.1093/jxb/erp387 Advance Access publication 2 February, 2010
This paper is available online free of all access charges (see http://jxb.oxfordjournals.org/open_access.html for further details)

Journal of Experimental Botany
www.jxb.oxfordjournals.org

RESEARCH PAPER

Modulating the light environment with the peach 'asymmetric orchard': effects on gas exchange performances, photoprotection, and photoinhibition

Pasquale Losciale[1,*], Wah Soon Chow[2] and Luca Corelli Grappadelli[1]

[1] Dipartimento Colture Arboree, University of Bologna, via Fanin 46, 40127 Bologna, Italy
[2] Research School of Biology, College of Medicine, Biology and Environment, The Australian National University, Canberra, Australian Capital Territory 0200, Australia

* To whom correspondence should be addressed: E-mail: plosciale@agrsci.unibo.it

Received 27 July 2009; Revised 11 December 2009; Accepted 11 December 2009

Abstract

The productivity of fruit trees is a linear function of the light intercepted, although the relationship is less tight when greater than 50% of available light is intercepted. This paper investigates the management of light energy in peach using the measurement of whole-tree light interception and gas exchange, along with the absorbed energy partitioning at the leaf level by concurrent measurements of gas exchange and chlorophyll fluorescence. These measurements were performed on trees of a custom-built 'asymmetric' orchard. Whole-tree gas exchange for north–south, vertical canopies (C) was similar to that for canopies intercepting the highest irradiance in the morning hours (W), but trees receiving the highest irradiance in the afternoon (E) had the highest net photosynthesis and transpiration while maintaining a water use efficiency (*WUE*) comparable to the other treatments. In the W trees, 29% and 8% more photosystems were damaged than in C and E trees, respectively. The quenching partitioning revealed that the non-photochemical quenching (*NPQ*) played the most important role in excess energy dissipation, but it was not fully active at low irradiance, possibly due to a sub-optimal *trans*-thylakoid ΔpH. The non-net carboxylative mechanisms (*NC*) appeared to be the main photoprotective mechanisms at low irradiance levels and, probably, they could facilitate the establishment of a *trans*-thylakoid ΔpH more appropriate for *NPQ*. These findings support the conclusion that irradiance impinging on leaves may be excessive and can cause photodamage, whose repair requires energy in the form of carbohydrates that are thereby diverted from tree growth and productivity.

Key words: Chlorophyll fluorescence, D1 protein, non-net carboxylative transports, non-photochemical quenching, photodamage, photosynthesis, quenching analysis, whole canopy gas exchange.

Introduction

The energetic basis of orchard productivity lies in the interaction between the tree and sunlight. The amount of dry matter produced by a tree is linearly related to the amount of light it intercepts (Monteith, 1977; Lakso, 1994). This concept drove the evolution of modern, intensive orchard systems (Corelli Grappadelli and Lakso, 2007), which aim to cover the ground as soon as possible with a photosynthetic surface in order to increase light interception, while maintaining good light distribution throughout the canopy, to improve fruit quality and flower bud differentiation (Palmer, 1980). Several authors have documented a direct relationship between planting density and fruit yield (t ha^{-1}) as a consequence of an increased leaf area index (*LAI*) and thus orchard light interception (Guerriero *et al.*, 1980; Hutton *et al.*, 1987; Chalmers and van den Ende, 1989; Loreti *et al.*, 1989; Caruso *et al.*, 2000; Corelli Grappadelli *et al.*, 2000; Nuzzo *et al.*, 2002). However, a direct relationship between irradiance and productivity is not always recorded. No difference for orchard yield was found, for example, on peach cv. Ross

© 2010 The Author(s).
This is an Open Access article distributed under the terms of the Creative Commons Attribution Non-Commercial License (http://creativecommons.org/licenses/by-nc/2.5), which permits unrestricted non-commercial use, distribution, and reproduction in any medium, provided the original work is properly cited.

trained as Cordon or Kearney Agricultural Center Perpendicular V (KAC-V) at 1196 trees per hectare, even though the Cordon training system intercepted more light than the KAC-V (Grossman and DeJong, 1998).

Light provides energy for electron transport, generating ATP and reducing power (NADPH) used in the Calvin–Benson cycle for carboxylation. Leaf net photosynthesis increases with irradiance until a saturation point is reached, beyond which no improvement is found for further increases in irradiance (Bohning and Burnside, 1956). The saturation point can be different between plant species and is affected by plant nutritional and water status, light environment during leaf growth, and leaf age. (Escalona *et al.*, 1999; Iacono and Sommer, 1999; Cheng *et al.*, 2001; Greer and Halligan, 2001). In peach (*Prunus persica* L.) the saturation point is normally reached at about 700–900 μmol photons m^{-2} s^{-1} (Kappel and Flore, 1983; Gaudillere and Moing, 1992). In several parts of the world, under clear sky conditions irradiance commonly reaches 2000 μmol photons m^{-2} s^{-1} or above (Nobel, 2005*a*); therefore, for photosynthesis at leaf level, about half the available light may be in excess (Corelli Grappadelli and Lakso, 2007). Ameliorating effects have actually been found in the photosynthetic performance of apple (*Malus*×*domestica* Borkh) and grapefruit (*Citrus paradisi* L.) by reducing (excessive) light interception with light-reflective kaolin particles sprayed on the leaves (Glenn *et al.*, 2001; Jifon and Syvertsen, 2003).

At the whole tree level, however, the saturation point is not always easily detectable. The genetically dwarf peach cv. Valley Red did not reach a steady-state when photosynthesis was measured on entire trees (Corelli Grappadelli *et al.*, 1996). On the other hand, in grapefruit, trees covered with 30% and 60% shading assimilated more dry matter than non-shaded ones (Raveh *et al.*, 2003). Whole plant gas exchange measurements carried out on apple trees sprayed with kaolin showed that, by reducing light and canopy temperature, net photosynthesis increased in response to the reduced environmental stress (Glenn *et al.*, 2003).

The energy absorbed by a leaf is managed through several competing pathways involving thermal processes, fluorescence, and photochemistry. The main purposes of these pathways are photosynthetic carboxylation and the dissipation of excess energy to limit the formation of reactive oxygen species (ROS). ROS react with and destroy a great number of the surrounding molecules (Niyogi, 1999). Light-dependent thermal dissipation, also called non-photochemical quenching (*NPQ*), can be divided into photoprotective quenching and photosystem II (PSII) photoinactivated re-emission (Björkman and Demmig-Adams, 1994; Müller *et al.*, 2001). The former is realized by the xanthophyll cycle and is able to dissipate up to 75% of the total absorbed energy (Demmig-Adams *et al.*, 1996). The key enzyme of this mechanism, violaxanthin de-epoxidase (VDE), is located in the thylakoid lumen and its activity is strictly dependent on the *trans*-thylakoid ΔpH (Ort, 2001). Maximum VDE activity is reached when the lumen pH is lower than 6.5 (Bratt *et al.*, 1995). A slowly reversible and *trans*-thylakoid ΔpH independent thermal dissipation (sustained *NPQ*), was found in some species and is attributable to a slow re-epoxidation of xanthophylls (Demmig-Adams, 1998). Although this slowly reversible down-regulation is usual in evergreen species or when high light is associated with low temperature; it is absent or very low in summer or in short-lived leaf species (Adams *et al.*, 2008; Demmig-Adams *et al.*, 2008). Photoinactivated PSII quenching is an uncontrolled process, caused by the thermal dissipation of excitation energy by photodamaged PSII complexes (Walters and Horton, 1993; Lee *et al.*, 2001; Müller *et al.*, 2001; Matsubara and Chow, 2004). Recent research suggests that this dissipation pathway might be considered as a slow, reversible, protective mechanism since damaged complexes can act as a light screen, protecting the surviving PSII from the light (Öquist *et al.*, 1992). Conversely, the remaining functional PSII are necessary to create the pH environment for new protein synthesis in the chloroplast, needed to repair photodamaged PSII (Sun *et al.*, 2006). This thermal dissipation contributes only to a small extent under normal circumstances because the damaged PSII complexes are quickly repaired (Mattoo *et al.*, 1984; Mattoo and Edelman, 1987; Aro *et al.*, 1994). The remaining absorbed energy is utilized to move electrons through several photochemistry processes, including photosynthesis. Electrons exiting the PSII core complex can be used to create reducing power for photosynthesis and photorespiration; they can otherwise be dissipated via alternative transports such as the water–water cycle, the cyclic transport around PSI, and the glutathione–ascorbate cycle (Niyogi, 1999). Moreover, these alternative pathways pump supplementary H^+ into the lumen to generate the proton gradient across the thylakoid membrane which supports VDE activity (Heber and Walker, 1992; Noctor and Foyer, 1998; Asada, 1999; Cruz *et al.*, 2005).

Despite such a wide range of photoprotective strategies, plants are not able to avoid photodamage. The main target for inactivation is the D1 protein (Aro *et al.*, 1993), which is one of two proteins comprising the PSII reaction centre. D1 is located in a region very rich in ^{3}Chl and, potentially, O_2: a perfect combination to generate ROS. This 'planned' destruction is used to avoid uncontrolled and widespread damage (Krieger-Liszkay, 2005), as plants have developed an effective, efficient, albeit energy-consuming mechanism for D1 recovery (Bottomley *et al.*, 1974; Eaglesham and Ellis, 1974; Anderson *et al.*, 1997). During the day the PSII pool can be almost entirely photoinactivated; a photon exposure of ~5 mol photons m^{-2} (to be compared with a photon exposure of about 30 mol photons m^{-2} over a sunny day) leads to the gross loss of about half of the active PSII (Chow and Aro, 2005). However, this is counteracted by rapid repair since there is no net loss of active PSII at the end of the day. Photoprotection and photoinactivation of PSII could be further increased by contingent thermal, water, and nutritional stresses (Powles, 1984; Miller *et al.*, 1995; Evans, 1996; Lee *et al.*, 1999; Baker and Rosenqvist, 2004). The dangerous consequences of a cascade from photo-oxidation to photoinactivation have caused plants to evolve towards a complex and

multi-pronged strategy for photoprotection and recovery with mutual support from the several processes involved. There is an energetic price to pay for this capability. These processes use reducing power and decrease net photosynthetic efficiency, since some intercepted photons are not used for carboxylation, but also because fixed CO_2 and reducing power are lost (Foyer and Harbinson, 1994).

Managing the energy captured by the tree is of great interest among scientists who look to increase the diminutive 5–10% of the absorbed energy in full light that plants are able to use for net carboxylation (Long *et al.*, 1994). In such a situation, even small changes in carboxylation efficiency and photosynthate allocation could modify the primary net and commercial plant productivity (Flore and Lakso, 1988).

The first objective of this study was to investigate, at the whole plant level, the relationship between the light environment and photosynthetic performance, water use, and PSII damage in peach. Once the response of the whole canopy carbon assimilation to irradiance was assessed, the study focused on the management of the absorbed energy, studying the partitioning of energy into the several utilization (i.e. net photosynthesis), and photoprotection pathways. This last investigation was performed only at a single leaf level since the energy partitioning approach at a whole canopy scale is still difficult.

Materials and methods

Plant material

The trials were carried out in 2006 at the University of Bologna Experiment Farm in Cadriano, Bologna, on three-year-old trees of the nectarine (*Prunus persica* (L.) Batsch var. *laevis*) cv. Alice col., grafted onto a GF305 rootstock with 5 m between the rows. The spacing is variable along the row, depending on the treatment. This cultivar exhibits a pillar growth habit naturally forming spindle-type canopies. The orchard is called 'asymmetric' because the rows vary in orientation and inclination, forming three different patterns of light interception during the day, two of which are asymmetric around solar noon. In addition to vertical, N–S (0–180°) oriented trees constituting the control (C), rows are either 330–150° (E) or 30–210° (W) oriented. The trees in the former are planted with canopies 30° slanting towards East, thus facing West, and trees from the latter are mirroring them, as they are planted with a canopy inclination 30° towards West, thus facing East (Fig. 1). The orchard consists of three plots, each containing one replicate of the three orientation/inclination combinations of 40–50 plants. Along the N–S oriented rows trees are spaced 1.2 m apart, and 1 m in the W and E treatments. The goal of this tree arrangement was to obtain three different light environments at the same time of day without modifying the overall climatic conditions.

Whole plant measurements

Two plants with similar vigour and crop load were chosen for each treatment. During fruit cell expansion (ST-III), when shoot growth had stopped, daily light interception was measured for each tree on a clear day using a custom-built light scanner (Giuliani *et al.*, 2000). The scanner was made up of a metal bar combining 48 irradiance sensors (NPN Silicon phototransistor P800, TRW Optron, TRW Inc., Carrolton, Texas, USA) spaced 0.05 m apart. Incoming irradiance was measured on unobstructed ground; subsequently, the scanner was moved under the tree, parallel to the row for a length encompassing all the area shaded by the canopy,

Fig. 1. Trees of the asymmetric orchard enclosed in whole plant chambers during the gas exchange measurements.

recording data every 0.2 m. Since the phototransistors used have a spectral response in the wavelength range 300–1100 nm, the fraction of light measured by the sensor in the visible light range (400–700 nm) was calculated according to Giuliani *et al.* (2000) in their Appendix 1. The irradiance measured by each sensor was considered as representative of the direct and diffuse irradiance falling on an area of 0.01 m^2 (0.05×0.2 m) surrounding that sensor. The difference between the incoming full light and that reaching the ground under the trees equals the total light flux intercepted by the plant (μmol photons m^{-2} s^{-1}).

Leaf area per tree was estimated by a calibration equation obtained by plotting area against dry weight of an increasing number of leaves for each tree. Before the end of the season all the leaves of each plant were detached while still full green and their dry weight was measured and converted to leaf area.

At ST-III and post-harvest (PHV), whole-canopy gas exchange was monitored using a custom-built open system, modelled after that described by Corelli Grappadelli and Magnanini (1993, 1997), with some modifications. Six polyethylene chambers were built, each enclosing one tree for 6 d and 8 d in ST-III and PHV, respectively. Air was forced through each assimilation chamber by a fan and the flow of air was measured by a custom-built flow gauge, calibrated using the standard gas method reported by Corelli Grappadelli and Magnanini (1993). The flow provided a full chamber volume exchange every 2–3 min, thus keeping the air temperature inside the chamber quite comparable to that outside (Corelli Grappadelli and Magnanini, 1993). Each flow gauge was connected to a CR10X datalogger (Campbell Scientific

Ltd. Leicestershire, UK), continuously monitoring the flow rate. A sample of gas from the inlet and outlet manifolds was drawn through PVC tubes to an infrared gas analyser (IRGA) (CIRAS SC, PP Systems, Hitchin, UK), for CO_2 (ppm) and H_2O (mbar) determination. The CR10X datalogger also controlled the operation of a bench of solenoid valves which switched the inlet and outlet flows from each chamber to the IRGA. A complete set of readings for each plant included the measurement of water vapour pressure and CO_2 concentration at the inlet and outlet of the chamber and the amount of air flowing through that chamber. Each plant was monitored every 15 min. Whole-canopy net carbon and water exchange rate was calculated by multiplying the CO_2 and H_2O differential between the inlet and the outlet of each chamber by the molar flow through the chamber (obtained from the measured flow, corrected for inlet air temperature). Dividing the gas exchange parameters by the total leaf area the specific net CO_2 uptake (*NCU*, μmol CO_2 m^{-2} s^{-1}), the specific transpiration (TR_{WP}, l H_2O m^{-2} h^{-1}) and the derived water use efficiency (*WUE*, mol l^{-1}) were obtained, and hourly averages were computed for each chamber. Since gas exchange parameters are strictly related to the environmental conditions (particularly to solar radiation), clear days with similar radiative profiles were chosen for the present analysis. Incident light energy density flux (W m^{-2}) was measured using a pyranometer attached to a weather station (AdCon telemetry GMBH, Austria) placed near the orchard.

To estimate the daily cumulative gross damage of PSII on each plant, fully expanded leaves, collected at predawn when almost all the PSII are fully functional, were used to calculate the quantum yield of photoinactivation (*Qy*). Leaf discs were floated with their abaxial side up, in order to facilitate gas exchange (Sun *et al.*, 2006), on a 1 mM lincomycin solution (an inhibitor of the D1 protein repair; Aro *et al.*, 1994) for 2 h in darkness. They continued to float with the abaxial side up on the lincomycin solution (23 °C) during illumination on the adaxial side at 800 and 1250 μmol photons m^{-2} s^{-1} for 0, 30, 60, 90, and 120 min; three leaf discs were used for each irradiance/time of exposure combination. On each disc the relative functional PSII amount was quantified by chlorophyll fluorescence as the maximum quantum yield of photosystem II (F_v/F_m), normalized to the value of the non-photoinhibited control, on both leaf sides after 45 min of dark adaptation (Losciale *et al.*, 2008) with a leaf fluorimeter attached to an open circuit infrared gas exchange system (Li-Cor 6400, Li-Cor Inc., Lincoln Nebraska USA). F_v is the variable fluorescence obtained as the difference between the maximal (F_m) and minimal (F_o) fluorescence for a dark-adapted leaf (Rosenqvist and van Kooten, 2003). A previous study comparing three methods for estimating the relative amount of the functional PSII on several plant species (Losciale *et al.*, 2008) demonstrated that, in peach, the average between F_v/F_m on both sides of the leaf, performed after 45 min of dark adaptation, gives a reliable estimation of the relative amount of the active PSII. Before the photoinhibitory treatment, six leaf discs (three for each irradiance) were used as non-photoinhibited controls. In these discs, the absolute functional PSII content (μmol PSII m^{-2}) was then quantified by flash-induced oxygen evolution (Chow *et al.*, 1989, 1991). Assuming that in the non-photoinhibited state the relative functional PSII amount is 1.0, and multiplying the relative functional PSII content of each leaf segment by the non-photoinhibited absolute amount of functional PSII (obtained by oxygen evolution measurements), the absolute functional PSII content can be calculated for each photoinhibition treatment. PSII activity decay depends on photon exposure, the product of irradiance and time of exposure (mol photons m^{-2}) according to the reciprocity law (Nagy *et al.*, 1995). The active PSII content decreases exponentially with the increase in photon exposure because the rate of photoinactivation depends on [active PSII] (Chow *et al.*, 2005). Since, in nature, nearly a complete recovery occurs continuously, the maximum slope of the exponential function represents maximum quantum yield (*Qy*) of photoinactivation of PSII (μmol PSII mol^{-1} photons). Multiplying *Qy* by the photon exposure intercepted per unit leaf area gives an estimation of the amount of damaged PSII (μmol PSII m^{-2}) over time (Hendrickson *et al.*, 2004). Daily cumulative PSII damage was estimated using the quantum yield of photoinactivation, the intercepted daily photon exposure and the total leaf area measured on each plant. This is a simplification as the *Qy* calculated at optimal and steady temperature in the laboratory may be an underestimation of the quantum yield of photoinactivation occurring in the field, where the photodamage process should proceed faster as the temperature stresses are greater (Yamamoto *et al.*, 2008).

Single leaf measurements

During fruit cell division (ST-I), stone hardening (ST-II), cell extension (ST-III), and post-harvest (PHV) six attached, well-exposed leaves were selected on the East and West side of C, W and E trees. Irradiance (μmol photons m^{-2} s^{-1}), leaf and air temperature (°C), gas exchange, and chlorophyll fluorescence parameters, used for the energy partitioning analysis, were measured on the leaves four times during the day (between 09.00 h and 17.00 h) using an open circuit infrared gas exchange system fitted with a leaf fluorimeter and a light sensor (Li-Cor 6400, Li-Cor inc., Lincoln Nebraska USA). Illumination was supplied by an artificial LED light source whose intensity was set equal to the natural irradiance measured next to the leaf lamina immediately before measurement. The maximum quantum yield of photosystem II (F_v/F_m) was measured predawn, after complete relaxation of the photosystems and after recovery during the night (Hikosaka *et al.*, 2004).

Analysis of the partitioning of excitation energy

Quenching analysis was carried out using the model by Hendrickson *et al.* (2004), combined with the photosynthesis model proposed by von Caemmerer (2000). Setting the total amount of energy absorbed by photosystems equal to 1.0:

$\Phi_{f,D}=F_s/F_m$ is the combined quantum efficiency of fluorescence and constitutive thermal dissipation, where F_s is the steady-state fluorescence for a light-adapted leaf and F_m is the maximum chlorophyll fluorescence after a saturating pulse for a dark-adapted leaf. Variations in irradiance do not alter this parameter appreciably (Hendrickson *et al.*, 2004);

$\Phi_{NPQ}=(F_s/F_m')-(F_s/F_m)$ is the quantum efficiency of light-dependent thermal dissipation, where F_m', is the maximum chlorophyll fluorescence after a saturating pulse for a light-adapted leaf. The light-dependent thermal dissipation is mainly promoted by the photoprotective non-photochemical quenching via the xanthophyll cycle and associated with the potential photoinactivated PSII;

$\Phi_{PSII}=1-(F_s/F_m')$ is the quantum efficiency of photochemical transports used for photosynthesis, photorespiration, mitochondrial respiration, and alternative transports (water–water cycle, cyclic transport around PSI, and the glutathione–ascorbate cycle).

To allow comparisons among all the energetic components, data were expressed as electron transport rates *J* (μmol e^- m^{-2} s^{-1}) by multiplying each quantum efficiency ($\Phi_{f,D}$, Φ_{NPQ}, Φ_{PSII}) by the estimated total amount of electrons that can be displaced by the absorbed irradiance:

$J_{TOT}=0.5\times0.85\times$irradiance, where the coefficient 0.5 takes into account that one electron is moved by two photons (one photon absorbed by each photosystem; Melis *et al.*, 1987) and 0.85 is the average leaf absorptance (Ehleringer and Pearcy, 1983; Krall and Edwards, 1992; Schultz, 1996).

Through gas exchange measurements, J_{PSII} could be partitioned into several components:

$J_{CO_2}=P_n\times4$ is the net photosynthesis expressed as electron transport rate, where P_n is the net carbon assimilation (μmol CO_2 m^{-2} s^{-1}) multiplied by four electrons sequestered for carboxylating one molecule of CO_2;

$J_{NC}=J_{PSII}-J_{CO_2}$ represents the residual absorbed energy used for non-net carboxylative processes such as photorespiration, alternative transports and dark respiration.

According to von Caemmerer (2000):

$$J_A=\frac{(P_n+R_d)\times(4C+8\Gamma^*)}{(C-\Gamma^*)}$$

is the rate of electron transport to photosynthesis and photorespiration, where R_d (μmol CO_2 m^{-2} s^{-1}) is the dark respiration, C is the chloroplast CO_2 concentration (μbar), and Γ* is the compensation point in the absence of mitochondrial respiration (μbar). Therefore

$J_{AT}=J_{PSII}-J_A$ represents the energy dissipated by alternative transports;

$J_R=J_A-J_{CO_2}$ represents the energy used for mitochondrial respiration and photorespiration.

Dark respiration was measured by placing the attached leaves in the dark and measuring the CO_2 exchange after stabilization. Chloroplast CO_2 concentration was calculated as C_i-P_n/g_i (von Caemmerer, 2000), where C_i is the intercellular CO_2 concentration, P_n is the rate of the net photosynthesis, and g_i is the internal diffusion conductance. A g_i of 0.35 mol m^{-2} s^{-1} was used as an average value found in the literature for peach leaves (Lloyd *et al.*, 1992; Ethier and Livingston, 2004). Correction for temperature dependence of g_i was made as detailed in Bernacchi *et al.* (2002). A photocompensation point (Γ*) of 38.6 μbar was chosen and it was corrected for the temperature by the Q_{10} factor (von Caemmerer, 2000).

To evaluate an ordered behaviour of the data collected on single leaves of the three treatments, a multivariate principal component analysis (PCA) was performed in order to identify the main sorting parameters and the possible cases gradients, using as variables: irradiance (*PPFD*), stomatal conductance (g_s, mol H_2O m^{-2} s^{-1}), transpiration (*Tr*, mmol H_2O m^{-2} s^{-1}), water use efficiency (*WUE*, mol CO_2 per litre of H_2O), air temperature (T_{air}), leaf temperature (T_{lf}), vapour pressure deficit (*VPD*, kPa), $J_{f,D}$, J_{NPQ}, J_{NC}, J_{CO2}, J_R, and J_{AT}.

Results

Whole trees

Light interception measurements were performed on July 7, a clear day, at 10.00, 11.00, 12.00. 13.30, 15.45, and 17.00 h. W trees increased their light interception during the morning, reaching the maximum value at 11.00 h, and later on W trees decreased their light interception and the lowest value was recorded at 17.00 h. E trees showed the minimum value at 10.00 h and their light interception gradually increased to a maximum at 17.00 h. In C trees the intercepted light was maximal at 10.00 h, slightly decreased until 12.00 h, and increased again in the afternoon reaching values similar to the morning. W trees intercepted more light than E and C till about 14.30 h. Then E canopies started to intercept more light and this difference was maintained until 17.00 h. Excluding measurements performed at 10.00 h and 17.00 h, control plants showed the lowest light interception throughout the day (Fig. 2).

Whole plant gas exchanges were measured from 8 July until 13 July in ST-III and from 14 July until 21 July after harvest. During fruit cell expansion, four days (10–13 July) were chosen while seven clear days (14–20 July) were selected in the post-harvest period. In ST-III the daily

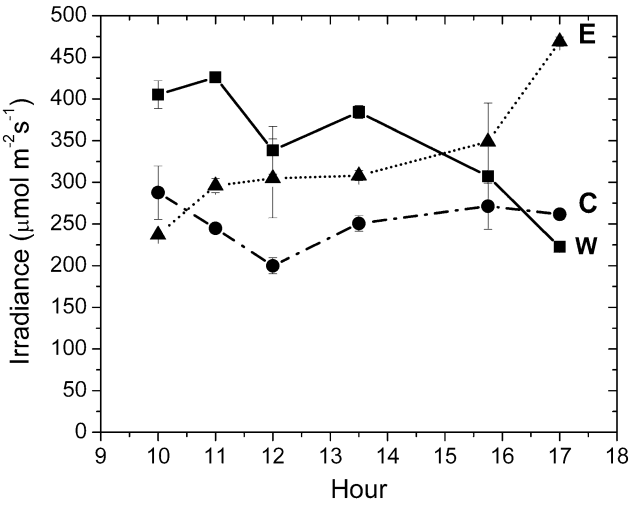

Fig. 2. Daily light interception pattern measured on W (closed squares), E (closed triangles), and C (closed circles) trees. Each point represents the average of two measurements ±SE.

patterns of net carbon uptake showed an increase for all treatments until 11.00 h with no differences revealed. The E treatment showed a further *NCU* increase, reaching the maximum value at 12.00 h and remaining at this level until 14.00 h, after which E net photosynthesis gradually decreased. W and C net CO_2 fixation diminished after 11.00 h and no difference was detected between these two treatments. C showed lower values than E at 12.00 h and at 13.00 h, while excluding values recorded at 15.00 h, W net photosynthesis was lower than E from 13.00 h until 17.00 h. At 18.00 h, *NCU* became similar among the three treatments (Fig. 3A). Transpiration (TR_{WP}) increased until 11.00 h without any difference among treatments. W canopies reached the maximum value at 11.00 h with a subsequent decrease during the afternoon, while C and E continued to increase their transpiration reaching the maximum at 14.00 h; afterwards, TR_{WP} decreased. Despite the fact that the maximum values were reached at two different times of the day, C and W transpiratory losses remained quite similar, even in the afternoon, and were lower than E until 14.00 h. Afterwards, a difference was recorded between E and W and, at 19.00 h, canopy transpiration was similar among treatments (Fig. 3B). Water use efficiency declined during the day, starting from the maximum value recorded at 06.00 h and reaching a steady-state at 12.00 h; no differences were recorded among treatments (Fig. 3C).

At post-harvest, net photosynthesis increased during the morning until 08.00 h, maintaining quite similar values until 10.00 h. No differences were recorded among treatments. After 10.00 h, net photosynthesis decreased in C and W canopies reaching minimum values at 18.00 h. At 15.00 h and at 16.00 h W net uptake was lower than C values (Fig. 3D). After 10.00 h, *NCU* of E trees continued to increase, reaching the maximum at 13.00 h; afterwards it decreased, reaching the minimum at 18.00 h. Excluding values recorded at 18.00 h, in the afternoon E trees showed higher *NCU* than the other two treatments (Fig. 3D). Whole

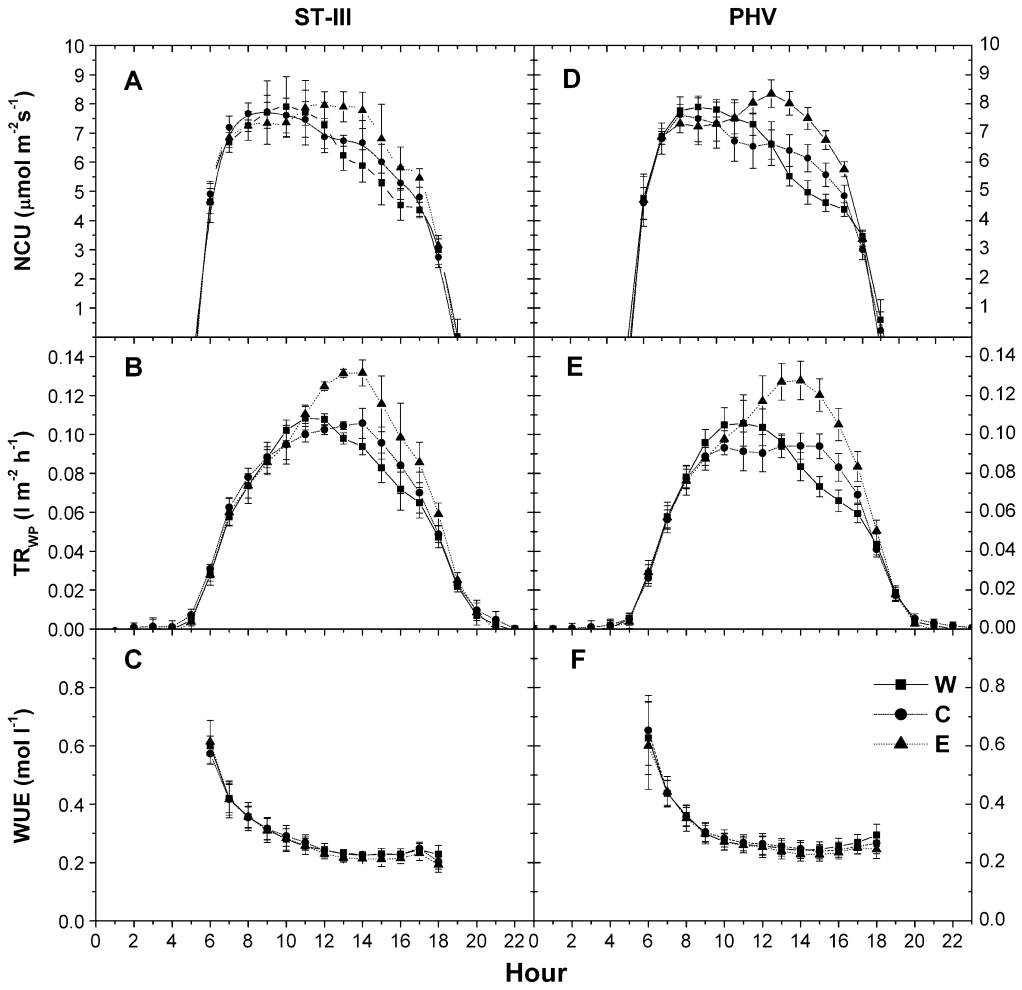

Fig. 3. Daily net carbon uptake (A, D), transpiration (B, E) and water use efficiency (C, F) pattern recorded in ST-III and PHV on W (closed squares), E (closed triangles), and C (closed circles) plants. Each point represents the average of 8–14 measurements ±SE.

canopy transpiration increased during the morning with no difference among the treatments. W reached the maximum value at 10.00–11.00 h; afterwards a rapid decrease was observed. In C trees TR_{WP} peaked at 10.00 h, maintained a steady-state until 15.00 h, and then decreased. Transpiration of E trees increased until 14.00 h, decreasing afterwards. In the afternoon, C transpiration was higher than W from 15.00 h until 17.00 h, although E trees showed the highest TR_{WP} (Fig. 3E). Also post-harvest, the water use efficiency was similar among treatments (Fig 3F). The maximum value was recorded in the early morning and decreased reaching a minimum, steady *WUE* at 12.00 h.

The functional PSII absolute content of non-photoinhibited samples was about 1.12 μmol PSII m^{-2}. This content of active PSII was sustained during the day, as photoinactivated PSII complexes were repaired quickly by D1 protein synthesis. Upon inhibiting the D1 protein synthesis, however, the functional PSII fraction decayed exponentially with an increase in photon exposure (data not shown); the calculated maximum quantum yield of photoinactivation of PSII (*Qy*) for a 100% active PSII population was 0.07 μmol PSII mol^{-1} photons. Multiplying this quantum yield of photoinactivation by the cumulative photon exposure through the day gives the cumulative gross content of photodamaged PSII. At each measurement, W trees showed a higher cumulative PSII damage than the other samples, while, in the morning, the inactive PSII centres were similar between C and E. In the afternoon, the increase in cumulative content of damaged PSII in E was more rapid, such that at 17.00 h the cumulative gross content of damaged PSII was 0.62, 0.44, and 0.57 μmol PSII m^{-2}, in W, C, and E samples, respectively, with the W trees having 8% and 29% more cumulative gross damage than E and C, respectively (Fig. 4).

Single leaves

Measurements were performed on 16 May, 12–13 June, 4–5 July, and 10 August in Stages I, II, III, and post-harvest, respectively. The irradiance changed during the day in the three canopies from ~150 to ~2100 μmol photons m^{-2} s^{-1}.

The multivariate principal component analysis (PCA) showed that the first two calculated eigenvalues explained data sorting by more than 80%. This percentage fell under 70% only in ST-III (Fig. 5). In the four stages a significant, positive relation was found among $J_{f,D}$, J_{NPQ}, J_{NC}, and irradiance (Fig. 5), and these four parameters heavily characterized the gradient represented by Factor I (factor

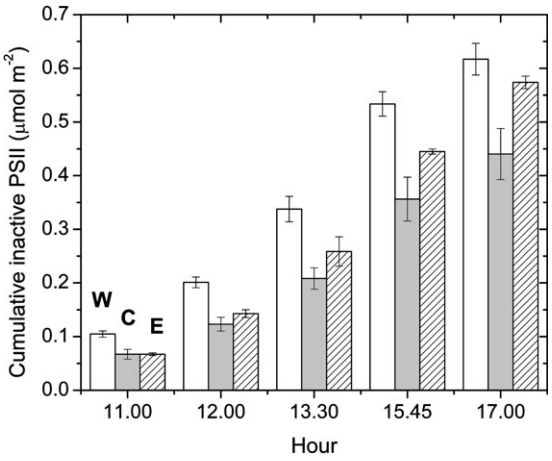

Fig. 4. Cumulative PSII inactivation estimated on W (white bars), E (dashed bars), and C (grey bars) trees. Each point represents the average of two measurements ±SE. The active PSII content for non-photoinhibited samples was about 1.12 μmol m^{-2}.

loading, r >0.9). This explained data sorting for more than 50% in all stages except ST-III (~45%). Stomatal conductance (g_s) was highly correlated to Factor 2 (r >0.8) except in Stage III, where g_s did not show any correlation with both principal components (Fig. 5C) and the calculated factor loadings were 0.4 and 0.2 for Factor 1 and 2, respectively. Air temperature, leaf temperature, and the vapour pressure deficit were more correlated to the second component than to Factor 1. T_{air}, T_{lf}, and *VPD* were positively related, while a negative correlation with stomatal conductance was found in ST-I, ST-II, and PHV (Fig. 5A, B, D). In all stages the correlation between J_{CO_2} and Factor 1 was higher than with the second. Although significant factor loadings (r >0.9) were recorded in ST-II and PHV, in the remaining two stages this parameter never exceeded 0.8. The J_{CO_2}/Factor 2 correlation was never significant; however, J_{CO_2}, J_R, and especially J_{AT} showed the highest correlation with Factor 2 among all electron transport rates (Fig. 5). The all measured cases projection on the main factor axes showed a strong

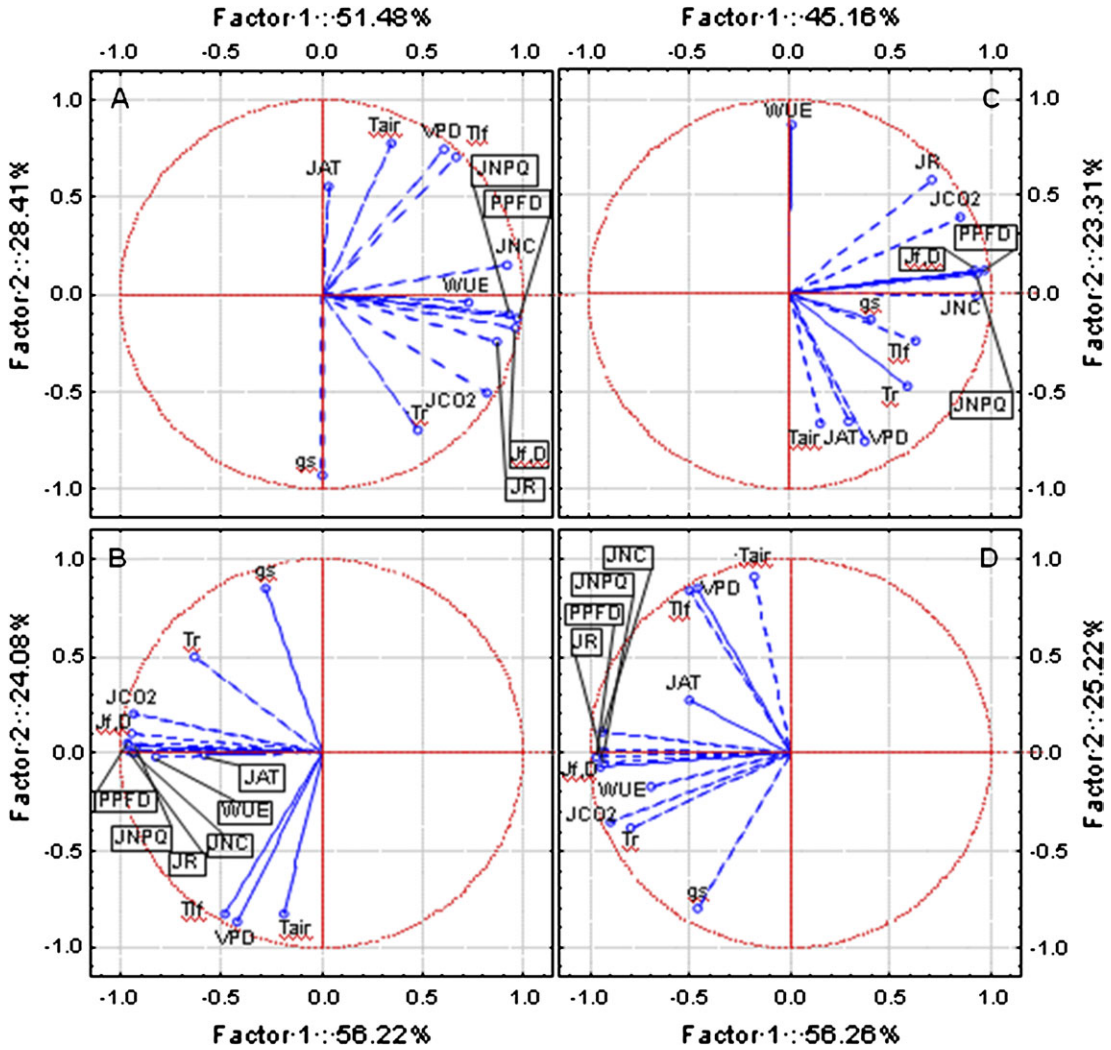

Fig. 5. Multivariate principal component analysis performed for ST-I (A), ST-II (B), ST-III (C), and PHV (D). Each of the 13 variables is represented by a vector, and its direction and length indicates the variable's contribution to the two principal factors. The longer and closer each vector is to the factor axis, the greater its contribution to determine the principal component.

overlapping between W, E, and C cases (Fig. 6). The three treatments did not influence the order of cases disposition along these gradients (Factor 1–2), therefore this classification was abandoned in order to study the general relationship existing between the J parameters and irradiance.

The energy used in the several dissipating processes was expressed as equivalent electron transport rate and plotted against irradiance for each stage. $J_{f,D}$ increased linearly with irradiance (Fig. 7), while in all the stages J_{NPQ} increased following an expo-linear pattern, with rapidly increasing response until 800–1000 μmol photons m^{-2} s^{-1}, when the maximum slope was attained and the energy dissipated as heat started to increase linearly with irradiance (Fig. 8). The rate of electron transport exiting PSII (μmol e^- m^{-2} s^{-1}) as a function of irradiance saturated at high irradiance for all the stages. The maximum slope was reached at the lowest irradiances and the electron transport rate used in photochemistry reached a saturation around 1000–1200 μmol photons m^{-2} s^{-1} (Fig. 9). Non-net carboxylative transports (J_{NC}) also increased with irradiance, reaching saturation at ~1000–1200 μmol photons m^{-2} s^{-1} and the maximum slope was recorded at low irradiance (Fig. 9). J_{CO_2} was directly related to irradiance. Function fitting applied to the data revealed a relevant scatter in ST-I (Fig. 9A). A similar pattern was followed in the remaining stages, although in ST-II (Fig. 9B) the relation had much less scatter (r^2=0.95). Generally, the electron transport rate effectively funnelled to net photosynthesis (J_{CO_2}) increased to a saturation point at about 1000–1200 μmol photons m^{-2} s^{-1} (Fig. 9). Partitioning J_{NC} allowed a calculation of the energy allocated to respiration/photorespiration (J_R) and to the alternative transports (J_{AT}). J_R was also directly related to irradiance. In ST-I and II a linear relation was recorded and a curvilinear one in ST-III. A curvilinear pattern was also found at post-harvest, although a considerable scatter was recorded (Fig. 10). In all the stages examined, the relation between the electron transport for the alternative transports (J_{AT}) and irradiance was not clear, although it increased reaching the highest values at middle-high irradiances (Fig. 10).

The integration of irradiance and the principal J parameters provided the amount of energy intercepted by leaves (Σ_{PPFD}) and devoted to photosynthesis ($\sum_{e-(CO2)}$) or to the main dissipative mechanisms ($\Sigma_{e\text{-}(f,D)}$, $\Sigma_{e\text{-}(NPQ)}$, and $\Sigma_{e\text{-}(NC)}$) between 09.00 h and 17.00 h in the three treatments during two of the stages (ST-III and PHV) which were also tested by the whole canopy measurements (Table 1). W leaves intercepted more light, but the electrons used for net fixation ($\sum_{e-(CO2)}$) were generally unchanged, except for C

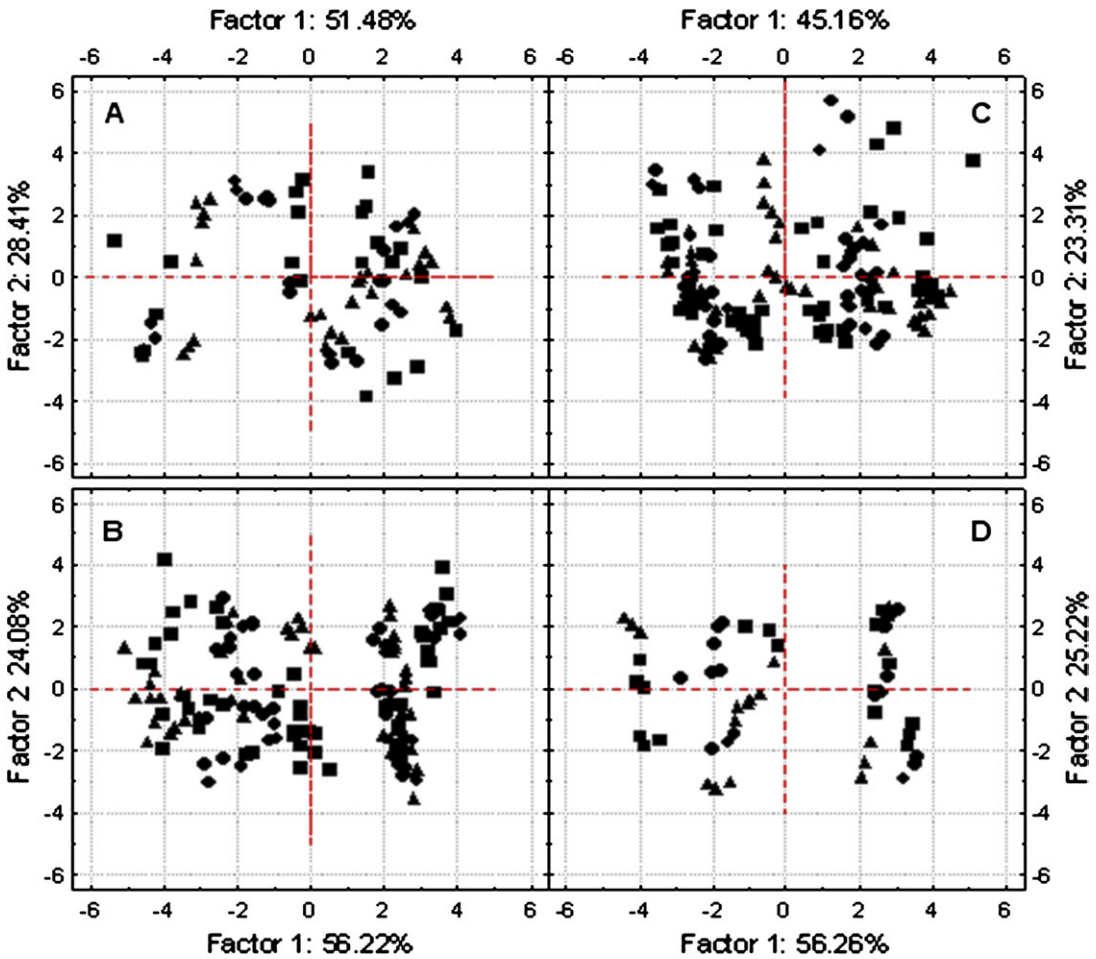

Fig. 6. Projection of W (closed squares), C (closed circles), and E (closed triangles) cases on the factor plane derived by the multivariate principal component analysis performed for ST-I (A), ST-II (B), ST-III (C), and PHV (D).

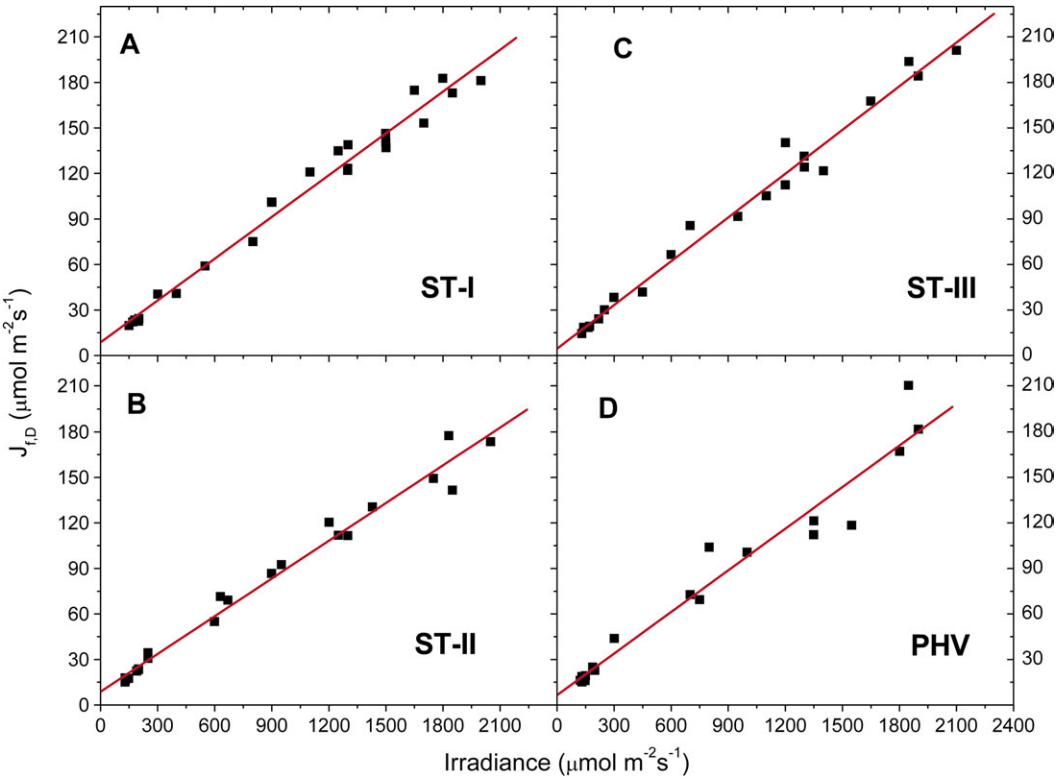

Fig. 7. Light response of fluorescence and constitutive thermal dissipation, $J_{f,D}$ ($y=ax+b$) recorded in ST-I (A), STII (B), ST-III (C), and PHV (D); The calculated r^2 was 0.98 in ST-I, II, III, and 0.95 in PHV. Each point represents the average of six leaves.

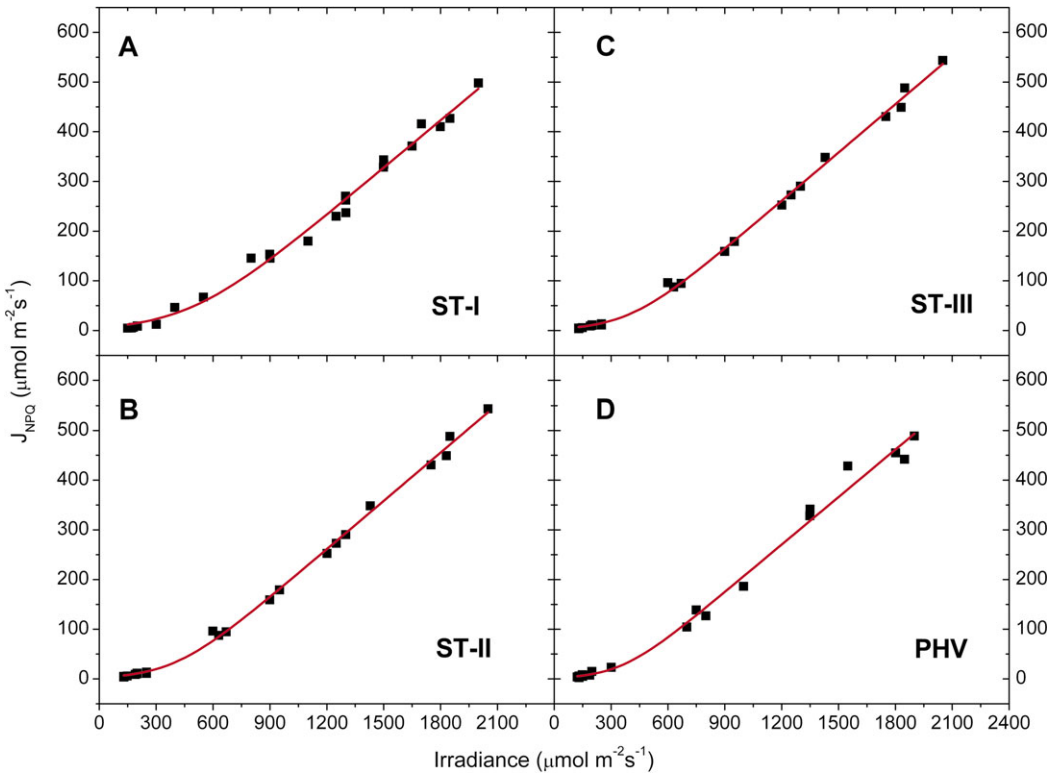

Fig. 8. Light response of: light dependent thermal dissipation of inactive PSIIs and promoted by xanthophyll cycle, J_{NPQ} ($y=(a/b)log(1+\exp[b(x-c)])$) recorded in ST-I (A), ST-II (B), ST-III (C), and PHV (D); The calculated r^2 was 0.99 in all investigated stages. Each point represents the average of six leaves.

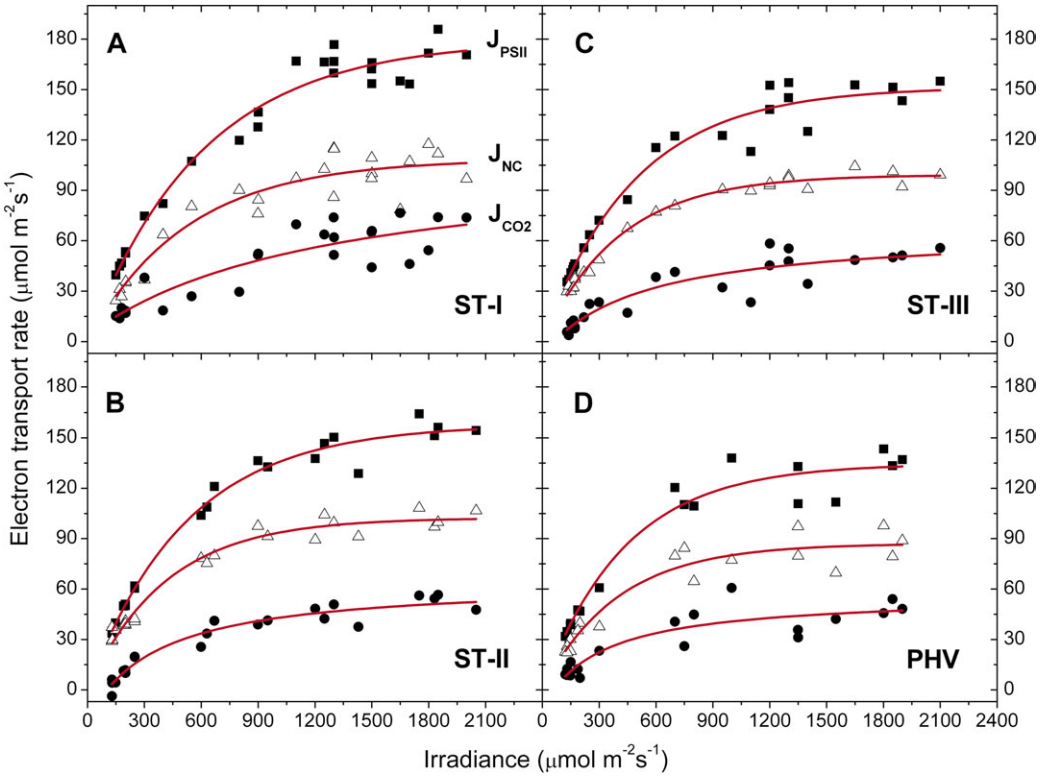

Fig. 9. Light response of photochemical electron transports exiting from PSII (closed squares), J_{PSII} ($y=a[1-\exp(-kx)]$); for non-net carboxylative transports (open triangles), J_{NC} ($y=a[1-\exp(-kx)]$); and effective electron transport for net photosynthesis (closed circles), J_{CO_2} ($y=y_0+ax/(b+x)$) recorded in ST-I (A), ST-II (B), ST-III (C), and PHV (D); The r^2 in ST-I, II, III, and PHV was 0.97, 0.99, 0.97, and 0.96 for the J_{PSII}/irradiance relation, 0.90, 0.97, 0.99, and 0.92 for the J_{NC}/irradiance curve and 0.79, 0.95, 0.85, and 0.81 for the J_{CO_2}/irradiance relation. Each point represents the average of six leaves.

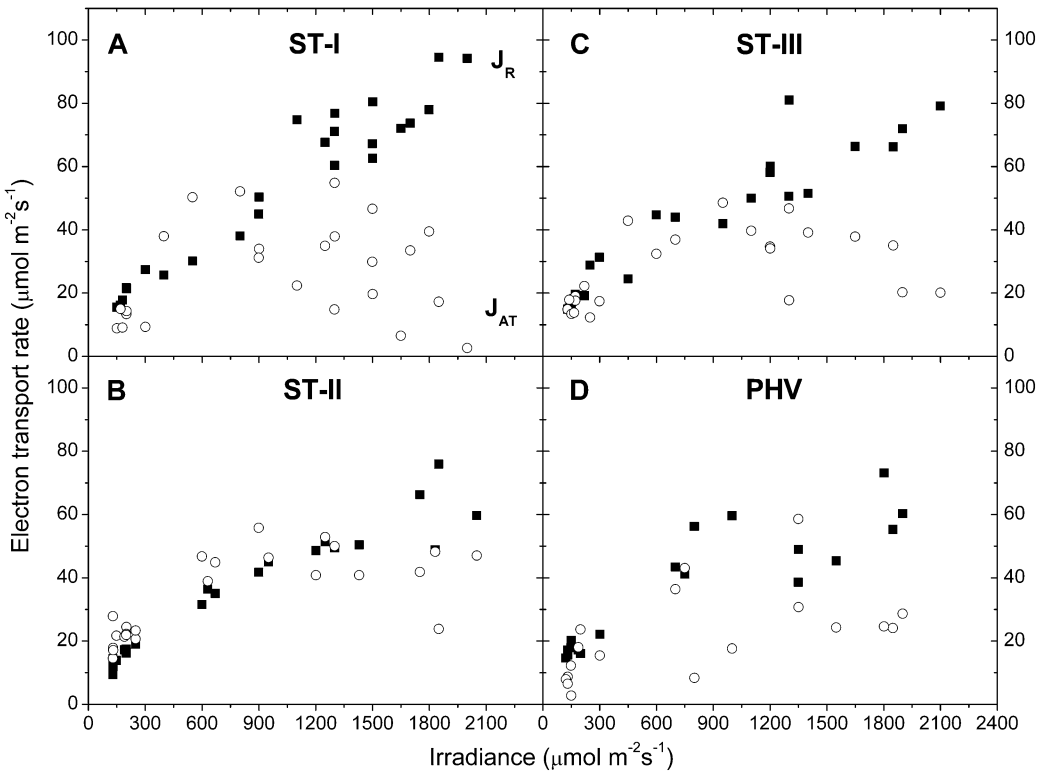

Fig. 10. Light response of electron transport rate for dark respiration and photorespiration (J_R, closed squares), and alternative transports (J_{AT}, open circles) recorded in ST-I (A), ST-II (B), ST-III (C), and PHV (D). Each point represents the average of six leaves.

samples at post-harvest, where $\sum_{e-(CO2)}$ was statistically lower than for E. Fluorescence and constitutive thermal dissipation ($\Sigma_{e\text{-}(f,D)}$), but above all non-photochemical quenching ($\Sigma_{e\text{-}(NPQ)}$), dissipated more energy in W samples, followed by E and C, respectively. Regardless of light interception, a similar energy amount was funnelled to the non-net carboxylative transports (Table 1).

Discussion

Whole trees

Canopy inclination and row orientation was varied to create three environments (under natural field conditions) which differed in the intensity and time of the day of peak light interception.

Daily patterns for gas exchange parameters were similar in ST-III and at post-harvest. In the morning, in spite of the differences in light interception recorded at this time, *NCU* and transpiration were similar among treatments. Available light did not limit net photosynthesis and, thanks to the favourable water and temperature status of the early daytime, stomatal conductance was not limiting in all treatments (Glenn *et al.*, 1999; Jifon and Syvertsen, 2003). At noon, while W light interception was still the highest, *NCU* and TR_{WP} started to decrease, suggesting a stomatal limitation rather than an influence of light (Fig. 3). In the afternoon, W light interception decreased while the opposite trend was followed by E and C plants. However, W canopies intercepted more light than E and C plants until 14.30 h (Fig. 2). Despite the lower light interception, E canopies showed a further *NCU* increase till 14.00 h, while net assimilation continued to decrease in C and W trees. As the evapotranspiration demand probably increased in the afternoon, plants responded with stomatal closure, which was followed by a reduction in photosynthesis (Fig. 3). The high irradiance experienced through most of the day by W trees possibly led to canopy temperature increases and to increases in the strictly related vapour pressure deficit (*VPD*). Stomatal closure can reduce water loss and net photosynthesis (Burrows and Milthorpe, 1976; Farquhar and Sharkey, 1982; Schulze, 1986). Compared to W plants, the E canopy inclination, via lower morning light interception, probably maintained canopy temperature to lower levels for longer during the day. Although *VPD* increased until 14.00 h, it did not seem to achieve values causing a reduction in stomatal conductance and *NCU*; as a result, the increased evapotranspiration demand could be met by increased transpiration, while the non-limiting light interception maintained *NCU* at higher values (Fig. 3). A similar behaviour was observed in apple by Glenn *et al.* (2003), who applied a highly reflective white particle film to tree canopies, reducing leaf temperature and stomatal limitation and increasing whole plant net assimilation.

In the afternoon, C transpiration increased until 14.00 h while *NCU* continued to decrease. Afterwards, stomatal closure became limiting even for transpiration and TR_{WP} started to decrease (Fig. 3). This stomatal closure was probably caused by the increasing evapotranspiration demand combined with the low light interception (Jarvis, 1976; Nobel, 2005*b*). After 15.00 h E water status and *VPD* probably became limiting, causing a decrease in stomatal conductance to reduce water loss and *NCU* as well, regardless of the irradiance increase (Fig. 3). Because higher photosynthetic levels were maintained in E plants, although they did transpire more water on a daily basis, their *WUE* was similar to the other treatments (Fig. 3).

Adding lincomycin to inhibit PSII recovery in leaf discs allowed us to observe the photoinactivation of PSII without the complication of concurrent repair. Assuming the same quantum yield of photoinactivation of PSII applied in conditions that permitted repair, the actual cumulative gross amount of photoinactivated PSII occurring during the day can be calculated from the daily photon exposure. W canopies, which intercepted the most light, showed the lowest daily CO_2 assimilation and the highest cumulative gross amount of damaged PSII: about 50% of the total PSII population in peach (Fig. 4). E plants had the highest photosynthetic performance and damage was 8% less than W. The lowest photon exposure was recorded in C plants with 29% lower PSII damage than W but similar daily CO_2 uptake (Fig. 4). However, this is an underestimation of the PSII damage occurring in the field as the *Qy* used was calculated at optimal and steady temperatures.

Table 1. Integrated (between 09.00 h and 17.00 h) mean values for incident irradiance (Σ_{PPFD}), absorbed energy used for net fixation ($\sum_{e-(CO2)}$) and dissipated via the fluorescence and constitutive thermal dissipation ($\Sigma_{e\text{-}(f,D)}$), the non-photochemical quenching ($\Sigma_{e\text{-}(NPQ)}$) and the non-net carboxylative transports ($\Sigma_{e\text{-}(NC)}$) measured four times per day during fruit cell expansion (ST-III) and post-harvest (PHV)

Each value is the average of 12 leaves per treatment (six per each side of the canopy) ±SE and was calculated by integration over time.

Stage	Trt	Σ_{PPFD} (mol photons m^{-2})	$\sum_{e-(CO2)}$ (mol e^- m^{-2})	$\Sigma_{e\text{-}(f,D)}$ (mol e^- m^{-2})	$\Sigma_{e\text{-}(NPQ)}$ (mol e^- m^{-2})	$\Sigma_{e\text{-}(NC)}$ (mol e^- m^{-2})
ST-III	C	24.04±0.01	0.96±0.14	2.34±0.15	4.79±0.15	2.13±0.10
	E	26.58±0.02	1.07±0.08	2.57±0.12	5.42±0.19	2.24±0.02
	W	28.81±0.01	0.89±0.11	2.84±0.24	6.29±0.19	2.22±0.12
PHV	C	21.18±0.02	0.81±0.11	2.07±0.03	3.95±0.14	2.17±0.11
	E	25.47±0.01	1.02±0.06	2.34±0.24	5.33±0.32	2.14±0.13
	W	27.82±0.01	0.90±0.08	2.62±0.19	6.03±0.25	2.27±0.20

Single leaves

As the whole canopy data pointed out differences in light management between treatments, single leaf measurements were performed within a range of natural (provided by the asymmetric orchard) irradiance of 150–2100 μmol photons m^{-2} s^{-1}.

The multivariate principal component analysis showed that all electron transport rates (J) were directly related to irradiance, as should be expected since they serve the purpose of dissipating the incoming energy (Fig. 5). Stomatal conductance (g_s), air (T_{air}) and leaf (T_{lf}) temperature, and vapour pressure deficit (VPD) were correlated with Factor 2, the former positively and the remaining parameters negatively. VPD is directly proportional to saturating vapour pressure and therefore to temperature; arguably, leaves coped with water loss by reducing stomatal conductance (Gindaba and Wand, 2007). The PCA analysis clearly showed that J_{CO_2} and J_{AT} were the most related to stomatal conductance and temperature among all the J parameters (Fig. 5), as shown by their correlation to the second principal component (Farquhar *et al.*, 1980).

The energy fraction ($\Phi_{f,D}$) dissipated by the combined fluorescence and constitutive thermal dissipation was constant at all irradiances as shown by the linear relation of $J_{f,D}$ with irradiance (Fig. 7). This almost constant thermal and fluorescence dissipation is the consequence of the exciton–radical pair equilibrium and the relatively slow electron transfer from pheophytin$^-$ to the primary quinone acceptor, compared with charge recombination to the excited state (Hendrickson *et al.*, 2004). Non-net carboxylative transports (J_{NC}) increased linearly with irradiance until 1000–1200 μmol photons m^{-2} s^{-1}, following, probably, an enzymatic first-order relation (Fig. 9). The enzymes involved in the cycles were fully activated and, as more electrons were moved by light, more electrons were dissipated via photochemistry. Above 1000–1200 μmol photons m^{-2} s^{-1} J_{NC} did not increase because the regeneration of electron carriers was probably limiting (Foyer and Harbinson, 1994). Even though non-net carboxylative transports are generally more dangerous than NPQ because of increased ROS formation during the intermediate steps, these mechanisms were first activated while J_{NPQ} responded to a limited extent to the medium-low irradiances (Fig. 8). The main mechanism involved in thermal dissipation is the strictly *trans*-thylakoid ΔpH-dependent xanthophyll cycle and the optimum lumen pH for violaxanthin de-epoxidase activity is under 6.5 (Bratt *et al.*, 1995). Probably, at medium-low irradiance, the thylakoid lumen was not sufficiently acidic to activate VDE completely. Leaves thus might have been able to dissipate the excess energy by alternative ways (Figs 8, 9). It is noteworthy that the water–water cycle, the cyclic transport around PSI, and the glutathione–ascorbate cycle are all able to increase the *trans*-thylakoid ΔpH, contributing to creating the optimal pH environment for VDE (Heber and Walker, 1992; Noctor and Foyer, 1998; Asada, 1999; Cruz *et al.*, 2005). Above 800–1000 μmol photons m^{-2} s^{-1}, lumen pH was probably optimal for VDE activation and J_{NPQ} started to increase linearly.

At all irradiance levels, and particularly above the photosynthetic saturation point, J_{CO_2} could not handle all the incoming energy, the excess of which had to be quenched by the other energy users, first of all non-photochemical quenching (Figs 8–9). Although a trend was generally apparent, a considerable scatter was nonetheless recorded (Fig. 9A, C, D), probably because, as shown in the PCA analysis, net photosynthesis was also related to temperature and stomatal conductance, in addition to irradiance (Farquhar *et al.*, 1980). J_R increased proportionally with irradiance never reaching a saturating point (Fig. 10). Although photorespiration consumes CO_2 it might be a necessary loss to deal with excess light or other environmental stresses (Osmond, 1981; Flexas *et al.*, 2002; Galmés *et al.*, 2007). The estimation of J_{AT} performed here is affected by leaf temperature, conductance, net photosynthesis (see PCA analysis), compensation point, and dark respiration, which in turn are easily influenced by the environment. This makes J_{AT} difficult to estimate (von Caemmerer, 2000) and probably explains why a clear pattern against irradiance was never found (Fig. 10).

The strong dependence of energy dissipation on non-photochemical quenching was further highlighted by the integration of the irradiance and the J parameters data collected at the leaf level (Table 1). In accordance with whole canopy observations, the higher amount of photons intercepted by W leaves did not promote an increase in carbon assimilation. On the contrary, excessive light was mainly dissipated by the ΔpH-dependent non-photochemical quenching. The contribution of the non-net carboxylative transports for energy quenching seemed to already achieve its steady-state in C leaves that had intercepted the lowest amount of photons (Table 1).

Conclusions

The 'asymmetric' peach orchard demonstrates that row orientation and canopy inclination can be used to provide, under natural conditions, quite diverse daily light interception profiles which allow the relationship among the absorbed light energy, photosynthetic performance, photoprotective strategies, and water use in the field to be studied.

Net carboxylation increased with irradiance until reaching a saturation point. Excess light that cannot enhance photosynthesis may impose water and thermal stresses, leading to the stomatal limitation of gas exchanges. Intercepting less light, C plants showed the lowest photoinhibition but equalled W in CO_2 uptake and water use. E trees assimilated more CO_2 and transpired more water than C and W, exhibiting an intermediate extent of PSII damage. The highest extent of cumulative gross photoinactivation of PSII was found in W trees in which the higher total light interception did not promote net carboxylation but proved to be in excess, exacerbating PSII damage. Since damaged photosystems are quickly repaired at the expense of energy (Chow and Aro, 2005; Nixon *et al.*, 2005), it would be important to investigate the cost of PSII recovery in terms of diminished whole-plant and/or fruit productivity.

The management of absorbed energy may be modulated by irradiance. At medium–low irradiance *NPQ* appeared limited, probably by a low *trans*-thylakoidal ΔpH, while net photosynthesis and the non-net carboxylative transports increased linearly with irradiance, reaching a steady state. These alternative pathways were the principal quenching mechanisms under low light and are probably used for creating the optimal *trans*-thylakoidal ΔpH for violaxanthin de-epoxidase functioning as well. At over-saturating light, when the xanthophyll cycle was fully activated, *NPQ* became the main dissipation pathway, probably supported by photorespiration.

Acknowledgements

The authors are greatly indebted to Drs L Manfrini, B Morandi, and M Zibordi for the pivotal contribution to data collection, Dr E Muzzi for the sharp suggestions in the statistical discussion, and Dr L Hendrickson for the critical reading of the manuscript. WS Chow is grateful for financial support from the Australian Research Council (DP0664719).

Appendix

List of abbreviations

C Chloroplast CO_2 concentration (μbar)

C_i Intercellular CO_2 concentration (μbar)

F_m Maximum chlorophyll fluorescence for a dark-adapted leaf

F'_m Maximum chlorophyll fluorescence for a light-adapted leaf

F_o Minimum chlorophyll fluorescence for a dark-adapted leaf

F_s Steady-state fluorescence

F_v Variable fluorescence (F_m–F_o)

F_v/F_m Maximum quantum yield of photosystem II (0–1, dimensionless)

g_i Internal diffusion conductance (mol m^{-2} s^{-1})

g_s Stomatal conductance (mol m^{-2} s^{-1})

J_A Electrons used for photosynthesis and photorespiration (μmol m^{-2} s^{-1})

J_{AT} Electrons used for the alternative transports (μmol m^{-2} s^{-1})

J_{CO_2} Net photosynthesis expressed as electron transport rate (μmol m^{-2} s^{-1})

$J_{f,D}$ Energy amount dissipated via the fluorescence and constitutive thermal dissipation, expressed as electron transport rate (μmol m^{-2} s^{-1})

J_{NC} Electrons used for the non-net carboxylative transports (μmol m^{-2} s^{-1})

J_{NPQ} Energy amount dissipated via the light dependent non-photochemical quenching, expressed as electron transport rate (μmol m^{-2} s^{-1})

J_{PSII} Electrons exiting from PSII (μmol m^{-2} s^{-1})

J_R Electrons used for mitochondrial respiration and photorespiration (μmol m^{-2} s^{-1})

J_{TOT} Absorbed irradiance expressed as electron transport rate (μmol m^{-2} s^{-1})

NCU Whole canopy net CO_2 carbon uptake (μmol m^{-2} s^{-1})

P_n Rate of net photosynthesis (μmol m^{-2} s^{-1})

PPFD Irradiance (μmol m^{-2} s^{-1})

Qy Quantum yield of photoinactivation (μmol PSII mol^{-1} photons)

R_d Dark respiration (μmol m^{-2} s^{-1})

T_{air} Air temperature (°C)

T_{lf} Leaf temperature (°C)

Tr Transpiration (mmol m^{-2} s^{-1})

TR_{WP} Whole canopy specific water transpiration (l m^{-2} h^{-1})

VPD Vapour pressure deficit (kPa)

WUE Water use efficiency (mol l^{-1})

Γ* Compensation point in the absence of mitochondrial respiration (μbar)

$\sum_{e-(CO2)}$ Mean integrated absorbed energy used for net fixation (mol e^- m^{-2})

$\Sigma_{e\text{-}(f;D)}$ Mean integrated absorbed energy dissipated via the fluorescence and constitutive thermal dissipation (mol e^- m^{-2})

$\Sigma_{e\text{-}(NC)}$ Mean integrated absorbed energy dissipated via the non net carboxylative transports (mol e^- m^{-2})

$\Sigma_{e\text{-}(NPQ)}$ Mean integrated absorbed energy dissipated via the non-photochemical quenching (mol e^- m^{-2})

Σ_{PPFD} Mean integrated incident irradiance (mol m^{-2})

$\Phi_{f,D}$ Quantum efficiency of fluorescence and constitutive thermal dissipation (0–1, dimensionless)

Φ_{NPQ} Quantum efficiency of the light-dependent non-photochemical quenching (0–1, dimensionless)

Φ_{PSII} Quantum efficiency of photochemical processes (0–1, dimensionless)

References

Adams III WW, Zarter CR, Much ZE, Amiard V, Demmig-Adams B. 2008. Energy dissipation and photoinhibition: a continuum of photoprotection. In: Demmig-Adams B, Adams WW III, Mattoo AK, eds. *Photoprotection, photoinhibition, gene regulation, and environment*. Dordrecht, The Netherlands: Springer, 49–64.

Anderson JM, Park YI, Chow WS. 1997. Photoinactivation and photoprotection of photosystem II in nature. *Physiologia Plantarum* **100,** 214–223.

Aro EM, McCaffery S, Anderson JM. 1994. Recovery from photoinhibition in peas (*Pisum sativum* L.) acclimated to varying growth irradiances (role of D1 protein turnover). *Plant Physiology* **104,** 1033–1041.

Aro EM, Virgin I, Andersson B. 1993. Photoinhibition of photosystem II. Inactivation protein damage and turnover. *Biochimica et Biophysica Acta* **1143,** 113–134.

Asada K. 1999. The water–water cycle. *Annual Review of Plant Physiology and Plant Molecular Biology* **50,** 601–639.

Baker NR, Rosenqvist E. 2004. Applications of chlorophyll fluorescence can improve crop production strategies: an examination of future possibilities. *Journal of Experimental Botany* **55,** 1607–1621.

Bernacchi CJ, Portis AR, Nakano H, von Caemmerer S, Long SP. 2002. Temperature response of mesophyll conductance. *Implications for the determination of rubisco enzyme kinetics and for limitations to photosynthesis in vivo. Plant Physiology* **130,** 1992–1998.

Björkman O, Demmig-Adams B. 1994. Regulation of photosynthetic light energy capture, conversion, and dissipation in leaves of higher plants. In: Schulze ED, Caldwell MM, eds. *Ecophysiology of photosynthesis*. Berlin, Germany: Springer, 17–47.

Bohning RH, Burnside CA. 1956. The effect of light intensity on rate of apparent photosynthesis in leaves of sun and shade plants. *American Journal of Botany* **43,** 557–561.

Bottomley W, Spencer D, Whitfeld PR. 1974. Protein synthesis in isolated spinach chloroplasts: comparison of light-driven and ATP-driven synthesis. *Archives of Biochemistry and Biophysics* **164,** 106–117.

Bratt CE, Arvidsson PO, Carlsson M, Åkerlund HE. 1995. Regulation of violaxanthin de-epoxidase activity by pH and ascorbate concentration. *Photosynthesis Research* **45,** 169–175.

Burrows FJ, Milthorpe FL. 1976. Stomatal conductance in the control of gas exchange. In: Kozlowski TT, ed. *Water deficits and plant growth*, Vol. IV. New York: Academic Press, 103–152.

Caruso T, Barone E, Di Vaio C. 2000. Factors affecting tree crop efficiency in young peach trees: rootstock vigour and training system. *Acta Horticulturae* **557,** 193–197.

Chalmers DJ, van den Ende B. 1989. Tatura trellis peaches: productivity over fifteen years. *Acta Horticulturae* **254,** 303–306.

Cheng L, Fuchigami LH, Breen PJ. 2001. The relationship between photosystem II efficiency and quantum yield for CO_2 assimilation is not affected by nitrogen content in apple leaves. *Journal of Experimental Botany* **52,** 1865–1872.

Chow WS, Aro EM. 2005. Photoinactivation and mechanisms of recovery. In: Wydrzynski T, Satoh K, eds. *Photosystem II: the light driven water:plastoquinone oxidoreductase.* Advances in Photosynthesis and Respiration, Vol. 22. Dordrecht, The Netherlands: Springer, 627–648.

Chow WS, Hope AB, Anderson JM. 1989. Oxygen per flash from leaf discs quantifies photosystem II. *Biochimica et Biophysica Acta* **973,** 105–108.

Chow WS, Hope AB, Anderson JM. 1991. Further studies on quantifying Photosystem II *in vivo* by flash-induced oxygen yield from leaf discs. *Australian Journal of Plant Physiology* **18,** 397–410.

Chow WS, Lee H-Y, He J, Hendrickson L, Hong Y-N, Matsubara S. 2005. Photoinactivation of photosystem II in leaves. *Photosynthesis Research* **84,** 35–41.

Corelli Grappadelli L, Giovannini D, Ravaglia R. 1996. Tipi di foglie e loro ruolo nella crescita dei frutti e nella produttività in peschi a diverso habitus vegetativo. Proceedings of 'Progetto Finalizzato Frutticoltura–Agro. Bio. Fruit'. *Cesena (Italy)* 10–11 May, 148–149.

Corelli Grappadelli L, Lakso AN. 2007. Is maximizing orchard light interception always the best choice? *Acta Horticulturae* **732,** 507–518.

Corelli Grappadelli L, Magnanini E. 1993. A whole-tree system for gas-exchange studies. *HortScience* **28,** 41–45.

Corelli Grappadelli L, Magnanini E. 1997. Whole-tree gas exchanges: can we do it cheaper? *Acta Horticulturae* **451,** 279–285.

Corelli Grappadelli L, Sansavini S, Stefanelli D, Asinelli A, Gaddoni M. . 2000. Forme di allevamento ed epoche di potatura del pesco per la bassa pianura padana. *Proceedings of XXIII Convegno Peschicolo,* Ravenna (Italy), 12–13 September 1997, 111–119.

Cruz JA, Avenson TJ, Kanazawa A, Takizawa K, Edwards GE, Kramer DM. 2005. Plasticity in light reactions of photosynthesis for energy production and photoprotection. *Journal of Experimental Botany* **56,** 395–406.

Demmig-Adams B, Adams III WW, Barker DH, Logan BA, Bowling DR, Verhoeven AS. 1996. Using chlorophyll fluorescence to assess the fraction of absorbed light allocated to thermal dissipation of excess excitation. *Physiologia Plantarum* **98,** 253–264.

Demmig Adams B, Ebbert C, Zarter CR, Adams III WW. 2008. Characteristic and species-dependent employment of flexible versus sustained thermal dissipation and photoinhibition. In: Demmig-Adams B, Adams WW III, Mattoo AK, eds. *Photoprotection, photoinhibition, gene regulation, and environment*. Dordrecht, The Netherlands: Springer, 39–48.

Demmig-Adams B, Moeller DL, Logan BA. 1998. **Adams III WW.** 1998. Positive correlation between levels of retained zeaxanthin+zeaxanthin and degree of photoinhibition in shade leaves of. *Schefflera arboricola. Planta* **205,** 367–374.

Eaglesham ARJ, Ellis RJ. 1974. Protein synthesis in chloroplasts. II. Light-driven synthesis of membrane proteins by isolated pea chloroplasts. *Biochimica et Biophysica Acta* **335,** 396–407.

Ehleringer JR, Pearcy RW. 1983. Variation in quantum yield for CO_2, uptake among $C_3$and C_4 plants. *Plant Physiology* **73,** 555–559.

Escalona JM, Flexas J, Medrano H. 1999. Stomatal and non-stomatal limitations of photosynthesis under water stress in field-grown grapevines. *Australian Journal of Plant Physiology* **26,** 421–433.

Ethier GJ, Livingston NJ. 2004. On the need to incorporate sensitivity to CO_2 transfer conductance into the Farquhar–von Caemmerer–Berry leaf photosynthesis model. *Plant, Cell and Environment* **27,** 137–153.

Evans JR. 1996. Developmental constraints on photosynthesis: effects of light and nutrition. In: Baker NR, ed. *Photosynthesis and the environment*. Dordrecht, The Netherlands: Kluwer Academic Publishers, 281–304.

Farquhar GD, Sharkey TD. 1982. Stomatal conductance and photosynthesis. *Annual Review of Plant Physiology* **33,** 317–345.

Farquhar GD, von Caemmerer S, Berry JA. 1980. A biochemical model of photosynthetic CO_2 assimilation in leaves of C_3 species. *Planta* **149,** 78–80.

Flexas J, Bota J, Escalona JM, Sampol B, Medrano H. 2002. Effects of drought on photosynthesis in grapevines under field conditions: an evaluation of stomatal and mesophyll limitations. *Functional Plant Biology* **29,** 461–471.

Flore JA, Lakso AN. 1988. Environmental and physiological regulation of photosynthesis in fruit crops. *Horticultural Review* **11,** 111–157.

Foyer CH, Harbinson J. 1994. Oxygen metabolism and the regulation of photosynthetic electron transport. In: Foyer CH, Mullineaux PM, eds. *Causes of photooxidative stress and amelioration of defence systems in plants*. Boca Raton FL: CRC Press, 1–42.

Galmés J, Abadia A, Cifre J, Medrano H, Flexas J. 2007. Photoprotection processes under water stress and recovery in Mediterranean plants with different growth forms and leaf habits. *Physiologia Plantarum* **130,** 495–510.

Gaudillere JP, Moing A. 1992. Photosynthesis of peach leaves: light adaptation, limiting factors and sugar content. *Acta Horticulturae* **315,** 103–109.

Gindaba J, Wand SJE. 2007. Climate-ameliorating measures influence photosynthetic gas exchange of apple tree. *Annals of Applied Biology* **150,** 75–80.

Giuliani R, Magnanini E, Fragassa C, Nerozzi F. 2000. Ground monitoring the light-shadow windows of a tree canopy to yield canopy light interception and morphological traits. *Plant, Cell and Environment* **23,** 783–796.

Glenn DM, Erez A, Puterka GJ, Gundrum P. 2003. Particle films affect carbon assimilation and yield in 'Empire' apple. *Journal of the American Society of Horticultural Science* **128,** 356–362.

Glenn DM, Puterka GJ, Drake S, Unruh TR, Knight AL, Baherle P, Prado E, Baugher T. 2001. Particle film application influences apple leaf physiology, fruit yield and fruit quality. *Journal of the American Society of Horticultural Science* **126,** 175–181.

Glenn DM, Puterka GJ, vanderZwet T, Byers RE, Feldhake C. 1999. Hydrophobic particle films: a new paradigm for suppression of arthropod pests and plant disease. *Journal of Economic Entomology* **92,** 759–771.

Greer DH, Halligan AE. 2001. Photosynthetic and fluorescence light responses for kiwifruit (*Actinidia deliciosa*) leaves at different stages of development on vines grown at two different photon flux densities. *Australian Journal of Plant Physiology* **28,** 373–382.

Grossman YL, DeJong TM. 1998. Training and pruning system effects on vegetative growth potential, light interception, and cropping efficiency in peach trees. *Journal of the American Society of Horticultural Science* **123,** 1058–1064.

Guerriero R, Loreti F, Morini S, Natali S. 1980. Eight years of observations on a peach double-row planted orchard. *Acta Horticulturae* **114,** 362–382.

Heber U, Walker D. 1992. Concerning a dual function of coupled cyclic electron transport in leaves. *Plant Physiology* **100,** 1621–1626.

Hendrickson L, Furbank RT, Chow WS. 2004. A simple alternative approach to assessing the fate of absorbed light energy using chlorophyll fluorescence. *Photosynthesis Research* **82,** 73–81.

Hikosaka K, Kato M, Hirose T. 2004. Photosynthetic rates and partitioning of absorbed light energy in photoinhibited leaves. *Physiologia Plantarum* **121,** 699–708.

Hutton RJ, McFadyen LM, Lill WJ. 1987. Relative productivity and yield efficiency of canning peach trees in three intensive growing systems. *HortScience* **22,** 552–560.

Iacono F, Sommer KJ. 1999. The measurement of chlorophyll fluorescence as a tool to evaluate the photosynthetic performance of grapevine leaves. *Acta Horticulturae* **493,** 31–44.

Jarvis PG. 1976. The interpretation of the variations in leaf water potential and stomatal conductance found in canopies in the field. Philosophical Transactions of the Royal Society of London. **B 273,** 593–610.

Jifon JL, Syvertsen JP. 2003. Kaolin particle film application can increase photosynthesis and water use efficiency of 'Ruby Red' grapefruit leaves. *Journal of the American Society of Horticultural Science* **128,** 107–112.

Kappel F, Flore JA. 1983. Effect of shade on photosynthesis, specific leaf weight, leaf chlorophyll content and morphology of young peach trees. *Journal of the American Society of Horticultural Science* **108,** 541–544.

Krall JP, Edwards GE. 1992. Relationship between photosystem II activity and CO_2 fixation in leaves. *Physiologia Plantarum* **86,** 180–187.

Krieger-Liszkay A. 2005. Singlet oxygen production in photosynthesis. *Journal of Experimental Botany* **56,** 337–346.

Lakso AN. 1994. Apple. In: Schaffer BB, Anderson PC, eds. *Handbook of environmental physiology of fruit crops*, Vol I. Boca Raton, FL: CRC Press, 3–42.

Lee HY, Chow WS, Hong YN. 1999. Photoinactivation of photosystem II in leaves of *Capsicum annuum. Physiologia Plantarum* **105,** 377–384.

Lee H-Y, Hong Y-N, Chow WS. 2001. Photoinactivation of photosystem II complexes and photoprotection by non-functional neighbours in *Capsicum annuum* L. leaves. *Planta* **212,** 332–342.

Lloyd J, Syvertsen JP, Kriedemann PE, Farquhar GD. 1992. Low conductance for CO_2 diffusion for stomata to the sites of carboxylationin leaes of woody species. *Plant, Cell and Environment* **15,** 873–899.

Long SP, Humphries S, Falkowski PG. 1994. Photoinhibition of photosynthesis in nature. *Annual Review of Plant Molecular Biology* **45,** 633–662.

Loreti F, Massai R, Morini S. 1989. Further observations on high density nectarine plantings. *Acta Horticulturae* **243,** 353–360.

Losciale P, Oguchi R, Hendrickson L, Hope AB, Corelli Grappadelli L, Chow WS. 2008. A rapid, whole-tissue determination of the functional fraction of Photosystem II after photoinhibition of leaves based on flash-induced P_{700} redox kinetics. *Physiologia Plantarum* **132,** 23–32.

Matsubara S, Chow WS. 2004. Population of photoinactivated photosystem II reaction centers characterized by chlorophyll *a* fluorescence lifetime *in vivo*. *Proceedings of the National Academy of Sciences, USA* **101,** 18234–18239.

Mattoo AK, Edelman M. 1987. Intramembrane translocation and posttranslational palmitoylation of the chloroplast 32-kDa herbicide-binding protein. *Proceedings of the National Academy of Sciences, USA* **84,** 1497–1501.

Mattoo AK, Hoffman-Falk H, Marder JB, Edelman M. 1984. Regulation of protein metabolism: coupling of photosynthetic electron transport to *in vivo* degradation of the rapidly metabolized 32-kilodalton protein of the chloroplast membranes. *Proceedings of the National Academy of Sciences, USA* **81,** 1380–1384.

Melis M, Spangfort M, Andersson B. 1987. Light-absorption and electron transport balance between photosystem II and photosystem I in spinach chloroplasts. *Photochemistry and Photobiology* **45,** 129–136.

Miller GW, Huang IJ, Welkie GW, Pushnik JC. 1995. Functions of iron in plants with special emphasis on chloroplasts and photosynthetic activity. In: Abadià J, ed. *Iron nutrition in soils and plants*. Dordrecht, The Netherlands: Kluwer Accademic Press, 19–28.

Monteith JL. 1977. Climate and the efficiency of crop production in Britain. *Philosophical Transactions of the Royal Society of London* **B 281,** 277–294.

Müller P, Li X, Niyogi KK. 2001. Non-photochemical quenching. A response to excess light energy. *Plant Physiology* **125,** 1558–1566.

Nagy L, Bálint E, Barber J, Ringler A, Cook KM, Maróti P. 1995. Photoinhibition and law of reciprocity in photosynthetic reaction of *Synechocystis* sp. PCC6803. *Journal of Plant Physiology* **145,** 419–415.

Nixon PJ, Barker M, Boehm M, de Vries R, Komenda J. 2005. FtsH-mediated repair of the photosystem II complex in response to light stress. *Journal of Experimental Botany* **56,** 357–363.

Niyogi KK. 1999. Photoprotection revisited: genetic and molecular approaches. *Annual Review of Plant Physiology and Plant Molecular Biology* **50,** 333–359.

Nobel PS. 2005*a*. Light. In: Sonnack K, ed. *Physiochemical and environmental plant physiology*. Burlington: Elsevier Academic Press, 180–182.

Nobel PS. 2005*b*. Leaves and fluxes. In: Sonnack K, ed. *Physiochemical and environmental plant physiology*. Burlington: Elsevier Academic Press, 357–359.

Noctor G, Foyer CH. 1998. Ascorbate and glutathione: keeping active oxygen under control. *Annual Review of Plant Physiology and Plant Molecular Biology* **49,** 249–279.

Nuzzo V, Dichio B, Xiloyannis C. 2002. Canopy development and light interception in peach trees trained to Transverse Y and Delayed Vase in the first four years after planting. *Acta Horticulturae* **592,** 405–412.

Öquist G, Chow WS, Anderson JM. 1992. Photoinhibition of photosynthesis represents a mechanism for the long-term regulation of photosystem II.. *Planta* **186,** 450–460.

Ort D. 2001. When there is too much light. *Plant Physiology* **125,** 29–32.

Osmond CB. 1981. Photorespiration and photoinhibition: some implication for the energetics of photosynthesis. *Biochimica et Biophysica Acta* **639,** 77–98.

Palmer JW. 1980. Computed effects of spacing on light interception and distribution within hedgerow trees in relation to productivity. *Acta Horticulturae* **114,** 80–88.

Powles SB. 1984. Photoinhibition of photosynthesis induced by visible light. *Annual Reviews in Plant Physiology* **35,** 15–44.

Raveh E, Cohen S, Raz T, Yakir D, Grava A, Goldschmidt EE. 2003. Increased growth of young citrus trees under reduced radiation load in semi-arid climate. *Journal of Experimental Botany* **54,** 365–373.

Rosenqvist E, van Kooten O. 2003. Chlorophyll fluorescence: a general description and nomenclature. In: DeEll JR, Tiovonen PMA, eds. *Practical applications of chlorophyll fluorescence in plant biology*. Boston: Kluver Academic Publishers, 31–77.

Schulze ED. 1986. Carbon dioxide and water vapour exchange in response to drought in the atmosphere and the soil. *Annual Reviews in Plant Physiology* **37,** 247–274.

Schultz HR. 1996. Leaf absorptance of visible radiation in *Vitis vinifera* L.: estimates of age and shade effects with a simple field method. *Scientia Horticulturae* **66,** 93–102.

Sun Z-L, Lee H-L, Matsubara S, Hope AB, Pogson BJ, Hong Y-N, Chow WS. 2006. Photoprotection of residual functional photosystem II units that survive illumination in the absence of repair, and their critical role in subsequent recovery. *Physiologia Plantarum* **128,** 415–424.

von Caemmerer S. 2000. Chlorophyll fluorescence and oxygen exchange during C_3 photosynthesis. In: CSIRO, Australia, ed. *Biochemical models of leaf photosynthesis*. CSIRO Publishing (Australia), 72–90.

Walters RG, Horton P. 1993. Theoretical assessment of alternative mechanisms for non-photochemical quenching of PSII fluorescence in barley leaves. *Photosynthesis Research* **36,** 119–139.

Yamamoto Y, Aminaka R, Yoshioka M, *et al*. 2008. Quality control of photosystem II: impact of light and heat stresses. *Photosynthesis Research* **98,** 589–608.